

CREEP RATCHETING BOUNDS BASED ON ELASTIC CORE CONCEPT

J. S. POROWSKI, W. J. O'DONNELL

O'Donnell Associates, Inc., 5100 Centre Avenue, Pittsburgh, Pennsylvania 15232, U.S.A.

ABSTRACT

The concept of an elastic core near the middle of the wall at any location in a component subjected to cyclic loading in the presence of creep was introduced by the authors to obtain bounds on the creep ratcheting strains at that location. The concept was quite useful since only elastic and creep strains could occur in the elastic core. Detailed solutions were obtained for elastic-perfectly plastic cylinders subjected to internal pressure and cyclic through-the-wall thermal stresses.

The present work includes isotropic and/or kinematic hardening effects and arbitrary temperature dependence of the yield strength of the material. The application of the bounds is extended to include loading histories with severe cycles resulting in plastic ratcheting. In general the relaxation of thermal stresses may result in a net accumulation of strain. The commonly used solution for complete relaxation between cycles does not include enhanced creep effects, and the latter are significant in many design applications.

A more general solution for partial relaxation of the core stress, σ_c , to an assumed level, σ_ℓ , is given in the present work. By bounding the enhanced creep effects for all subsequent cycles, and the strains due to the partial relaxation, the authors have developed bounds which can be optimized using arbitrarily selected values of the relaxation level, σ_ℓ .

Energy dissipation concepts are used to bound the accumulated strains due to relaxation within each cycle. The strains due to relaxation, δ , are shown to be bounded by:

$$\delta \leq \frac{\sigma_c^2 - \sigma_\ell^2}{E\sigma_\ell}$$

The total inelastic strain accumulation is the sum of the creep strains which can be determined from isochronous curves for each cycle at σ_ℓ stress; plus the strain increments, δ , due to stress relaxation, and the plastic ratchet strain increments.

Generalized core stress graphs are given to facilitate design applications.

NOMENCLATURE

- a, b - distances between mid-plane of the wall and the elastic-plastic interfaces for low-temperature stress extreme of the cycle (Figure 1)
- $B = \frac{S_{Y_T} - S_{Y_C}}{2}$ - translation of the yield surface origin (Figure 1)
- $C = \frac{S_{Y_T} + S_{Y_C}}{2}$ - average yield strength for tension and compression
- c - distance between mid-plane of the wall and the elastic-plastic interface for the case when captive plastic cycling occurs in stress regime P (Figure 1)
- d - thickness of the wall
- E - elastic modulus
- S_{Y_0} - yield strength of the virgin material
- S_{Y_C} - yield strength in compression for hardening material
- S_{Y_T} - yield strength in tension for hardening material
- α - coefficient of thermal expansion
- σ, z - coordinate system (Figure 1)
- $v(n)$ - creep strain incurred at constant stress within a cycle (n)
- $\delta(n)$ - upper bound on inelastic strain incurred due to relaxation within a cycle (n)
- $\epsilon(n)$ - total inelastic strain increment within a cycle (n)
- $\eta(n)$ - plastic strain increment within a cycle (n)
- ν - Poisson's ratio
- σ - stress in a uniaxial model defined for the hoop direction of a cylindrical vessel
- $\sigma_c < S_y$ - elastic core stress shown in Figure 1
- $\{\sigma_c\} \geq S_y$ - nominal σ_c values resulting from Eqs. (6), (7) in plastic ratcheting regimes (R)

- σ_l - intermediate relaxation level of σ_c stress
- σ_p - primary, pressure-induced membrane stress
- σ_t - secondary, thermally-induced stress
- $\sigma'_p, \sigma'_t, \sigma'_c, \sigma'_l$ - normalized stresses

Subscripts L, H define low- and high-temperature stress extremes of the cycle (cold and hot ends, respectively).

Subscript o defines the conditions for virgin material.

INTRODUCTION

Upper bounds on accumulated strains in cylindrical shells subjected to sustained pressure and cyclic thermal stresses in the creep regime were derived in Ref. [1]. These bounds are for elastic-perfectly plastic material with temperature-independent yield properties. The applicability of the bounds was limited to cycling below the plastic ratcheting regime.

These bounds are extended herein to include arbitrary work-hardening, temperature-dependent yield properties, and severe cycling into the plastic ratcheting regime.

The concept of partial relaxation of the elastic core stresses is introduced herein to obtain a unified solution for load histograms which include severe cycles into the plastic ratcheting regime. The maximum energy available for dissipation within a cycle is used to bound the corresponding inelastic strain increment due to relaxation and redistribution of stresses through the wall.

The bounds derived herein allow the designer to take credit for the higher residual stresses which can be retained during shutdown because of the higher yield strength of the material at low temperature, and for the beneficial effects of hardening (kinematic or isotropic) in reducing the ratcheting strains. Moreover, the effects of a limited number of severe cycles with subsequent operation in the creep regime are efficiently bounded. As in Ref. [1], the uniaxial model is used herein to obtain conservative bounds. Only a review of the solutions and portions of the proofs needed to understand the basic concepts are given. The complete paper will be published.

THE BASIC ANALYTICAL MODEL

A complete description of the uniaxial model used to bound accumulated strains in the creep regime is given in Ref. [1]. Typical stress profiles for the cold and hot extremes of the thermal cycle are shown in Figures 1a herein. The graph in Figure 2, defines the stress regimes resulting in elastic behavior (E), shakedown (S_1 and S_2), captive plastic cycling (P), and

plastic ratcheting (R_1 and R_2).

Creep occurs only at the hot end of the thermal cycle. The Tresca yield condition is used throughout the analysis, and the dominating hoop component of the pressure-induced stress is considered in the uniaxial model. For a temperature difference ΔT through the wall, the thermal stress in the constrained wall is:

$$\sigma_t = \frac{\alpha E \Delta T}{2(1 - \nu)} \quad (1)$$

where α is the thermal expansion coefficient, E is Young's modulus, and ν is Poisson's ratio.

The pressure stress σ_p is uniformly distributed through the wall. For simplicity, a linear distribution of the thermally-induced stress σ_t is assumed. The σ_p stress is sustained through the cycle. The thermal stress ranges from zero to maximum at the extremes of the cycle.

A similar uniaxial model was first introduced by Bree [2], [3], to analyze the pressurized fuel can. The authors developed the elastic core concept for this model in order to obtain upper bounds for creep ratcheting in Ref. [1]. Energy concepts are used herein to extend the applicability of the bounds to include intermittent cycling in the plastic ratcheting regime.

EFFECTS OF YIELD STRENGTH VARIATIONS

The effect of having a different yield strength in compression, S_{Y_C} vs. tension, S_{Y_T} , was considered in Ref. [4]. As indicated in Ref. [4]*, the iso-strains given in Figure 2 can be generalized for any yield strengths by normalizing the variables σ_p and σ_t as

$$\sigma'_p = \frac{2\sigma_p - (S_{Y_T} - S_{Y_C})}{S_{Y_T} + S_{Y_C}} \quad (2)$$

$$\sigma'_t = \frac{2\sigma_t}{S_{Y_T} + S_{Y_C}} \quad (3)$$

Geometrically, as shown in Figure 1b, the normalized coordinate system is shifted along σ axis by the quantity $B = 1/2 (S_{Y_T} - S_{Y_C})$, which defines the translation of yield surface origin for hardening materials. The magnitude of the entering quantities is normalized by the modulus $C = 1/2 (S_{Y_T} + S_{Y_C})$, which determines the size of the current yield surface. The normalized core stress is then:

$$\sigma'_C = \frac{2\sigma_C - (S_{Y_T} - S_{Y_C})}{S_{Y_T} + S_{Y_C}} \quad (4)$$

*Compare: $2S_Y - \sigma_m$ in Fig. 12 of Ref. [4] equals to $(S_{Y_T} + S_{Y_C})$ herein where σ_m corresponds to $(S_{Y_T} - S_{Y_C})$.

and thus

$$\sigma_c = \frac{1}{2}[\sigma'_c(S_{Y_T} + S_{Y_C}) + (S_{Y_T} - S_{Y_C})] \quad (5)$$

The resulting isostrains $\sigma'_c = \text{const.}$ plotted using normalized coordinates and absolute values of σ'_p and σ'_t are identical to those given in Ref. [1] for non-hardening materials. The relations governing the dimensionless core stress σ'_c and the locations of elastic-plastic interfaces in steady stress cycling involve only normalized quantities and therefore remain unchanged as in Ref. [1]:

$$\sigma'_c = 1 + \sigma'_t - 2\sqrt{\sigma'_t(1 - \sigma'_p)} \quad \text{in Regime } S_1 \quad (6)$$

$$\sigma'_c = \sigma'_p \sigma'_t \quad \text{in Regimes } S_2 \text{ and } P \quad (7)$$

$$a = (1 - 2\sqrt{(1 - \sigma'_p)/\sigma'_t}) d/2 \quad \text{in Regime } S_1 \quad (8a)$$

$$a = (\sigma'_p - 1/\sigma'_t) d/2 \quad \text{in Regimes } S_2, P \quad (8b)$$

$$b = (\sigma'_p + 1/\sigma'_t) d/2 \quad \text{in Regimes } S_2, P \quad (9)$$

$$c = (1/\sigma'_t)d \quad \text{in Regime } P \quad (10)$$

where the notation is explained in Figure 1. Equations (8b) and (9) are applicable also in the Regimes R_1 and R_2 respectively.

EFFECTS OF STRAIN HARDENING

The yield strengths in tension and compression may be determined using the accumulated strains evaluated for the preceding cycles. For isotropic hardening, results can be obtained simply by sequentially adjusting the yield strength. For kinematic hardening and mixed hardening mode cases, the results can be obtained by employing the solution given in the previous section. Figure 3 shows the effect of a gradual translation of the yield surface on the magnitude of the stress in the elastic core σ_c . The relation for the core stress in kinematically-hardened materials relative to the initial value for virgin material can be obtained using Equation (5) for both the virgin and hardened materials:

$$\sigma_c/\sigma_{c_0} = (\sigma'_c + B/S_{Y_0})/\sigma'_{c_0} \quad (11)$$

where subscript zero is related to virgin material.

As can be seen in Figure 3, kinematic hardening of the material lowers the stress in the elastic core, tending to reduce subsequent creep strains. The stress profiles in Figure 3 are given for constant pressure stress $\sigma_p = 0.6 S_{Y_0}$ and thermal stress $\sigma_t = 1.2 S_{Y_0}$, and stepwise dislocation of the yield surface indicated by letters A, B, C and D. For kinematic hardening, relations (2) and (3) reduce to:

$$\sigma'_p = (\sigma_p - B)/S_{Y_0} \quad (12a)$$

$$\sigma'_t = \sigma_t/S_{Y_0} \quad (12b)$$

and the relation (5) simplifies to yield:

$$\sigma_c = \sigma'_c S_{Y_0} + B \quad (12c)$$

EFFECTS OF TEMPERATURE-DEPENDENT YIELD PROPERTIES

The stress profiles in Figure 1 are shown for the simple case where the yield strength is independent of temperature. The core stress σ_c during the hot operating period is obviously affected by the residual stresses which exist at the cold extreme of the cycle. A high yield strength in the cold shut-down condition will permit the development of high favorable residual stresses which reduce the hot operating stresses. Thus, the correct core stress can be obtained using the low temperature yield strength in the previous solution for temperature-independent properties, provided that this calculated core stress does not exceed the hot yield strength:

$$\sigma_c \leq S_{Y_H} \quad (13)$$

The stress profiles for such a case in stress regimes S_1 and S_2 are shown in Figures 4a and 4b, respectively. In the stress regime S_1 , the surface stress on the side A of the wall, which flows plastically within the initial cycle, is governed by the simple relation:

$$\sigma_A = \sigma_t - S_{Y_L} \quad (14)$$

σ_A is always lower than the elastic core stress σ_c which occurs at the surface B. For regime S_2 , the stress profiles in the outer layers are anti-symmetric, and plastic flow of the picks on both sides does not affect the core stress level provided condition (13) is satisfied.

If the elastic core stress falls between the yield strength at the low- and high-temperature extremes of the cycle, i.e.,

$$\text{if: } S_{Y_H} < \sigma_c < S_{Y_L} \quad (15)$$

the stress is redistributed during the heating-up period as shown in Figure 5a and 5b for regimes S_1 and S_2 , respectively. The resulting plastic increment is due to further extension in the elastic layer $z < a$ plus the strain generated by the reduction of elastic stress in layer $z > a$ which flows plastically during heat-up.

$$\text{Then: } \eta = [(\sigma_{c_L} - S_{Y_H}) + (\{\sigma_c\}_H - S_{Y_L})]/E \quad (16)$$

where the stresses σ_{c_L} and $\{\sigma_c\}_H$ can be obtained from Eqs. (6) or (7). The yield strengths S_{Y_L} and S_{Y_H} should be used to normalize the stresses σ_p and σ_t . The brackets $\{\}$ enclosing σ_c are used only to distinguish calculated σ_c values

which are larger than the hot yield strength S_{YH} and have not been corrected to account for yielding. For the considered case determined by condition (15), the plastic strain increment of the middle plane of the wall occurs only at the hot end of the cycle.

The elastic-plastic interfaces (a, b, c) may be obtained using the relations (8) through (10) with σ_p and σ_t normalized for cold and hot extremes of the cycle.

EFFECTS OF CYCLES IN THE PLASTIC RATCHETING REGIME

The concept of using the nominal values of elastic core stress $\{\sigma_c\} > S_Y$ or $\{\sigma'_c\} > 1$ for evaluation of plastic strain increments introduced in the previous section can be generalized to include the plastic ratcheting regimes. Figures 6a and 6b show the stress profiles for regimes R_1 and R_2 , respectively. For constant yield strength within the cycle as shown in Figure 6a, the plastic strain increments incurred during shutdown and subsequent heat-up are identical. The total strain increment incurred within the cycle is then

$$\eta = 2[\{\sigma_c\} - S_Y]/E \quad (17)$$

The location of the elastic-plastic interfaces (a, b) can be obtained from Eqs. (8) and (9). The interface governed by parameter \underline{a} occurs now on the other side of the mid-plane, which is subject to plastic yielding at each end of the cycle. The parameter \underline{c} is not applicable in the R regimes.

The case of different yield strengths at both ends of the cycle is shown in Figure 6b. The plastic increments on both extremes of the cycle are not the same, and the total plastic strain is governed by the relation analogous to that obtained previously for the S regimes:

$$\eta = [(\{\sigma_c\}_L - S_{Y_L}) + (\{\sigma_c\}_H - S_{Y_H})]/E \quad (18)$$

In fact, the relations (16) and (18) are essentially identical except for the different notation σ_{cL} and $\{\sigma_c\}_L$ used for the real and nominal core stress in the S and R regimes, respectively. Thus, the total plastic strain increment can be obtained without distinguishing between the stress regimes resulting in plastic increments at one end or both ends. The σ_c and $\{\sigma_c\}$ values can be conveniently obtained from the diagram in Figure 2.

BOUNDS ON ENHANCED CREEP FOLLOWING PLASTIC RATCHETING

The histograms for most structural components, often contain a few cycles which are essentially more severe than the majority of others. Even if these few cycles result in a significant inelastic strain increments, the integrity of the structure may still be adequate since the total accumulated inelastic strain may not be too large. For cycles in the plastic ratcheting regime, yielding affects the entire thickness of the wall and the concept presented in Ref. [1] cannot be directly applied. Moreover, for cycles remaining in the shakedown regime but resulting in calculated maximum elastic core stresses near yield, the creep strain from the isochronous curves is high and the bound

of Ref. [1] becomes essentially less effective.

In order to obtain more efficient bounds the concept of partial relaxation of the core stress is introduced herein. In the creep regime, the stress field tends asymptotically to the stationary state related to sustained primary loads. For the cylindrical tube considered herein, full relaxation of residual stresses results in a uniform pressure stress σ_p . For the case where only partial relaxation occurs, as shown in Figure 1, the central horizontal portion of the stress profile remains uniform. The stress distribution in the outer layers becomes complex. The horizontal portion of the profile is maximized at the beginning of the operating period. For $\sigma_c < 1.0$ the center layer remains elastic and the maximum stress is σ_c . For $\{\sigma_c\} \geq 1$ the stress in the horizontal part of the profile reaches the yield limit, S_{YH} , at the hot end of the cycle.

For any given histogram of cyclic loading, the middle plane stress can be plotted for critical locations in the component, as shown in Figure 7. For each cycle, the strain increment can be evaluated as the sum of the inelastic strain due to stress relaxation from σ_c to σ_ℓ , plus the creep strain $v_{(n)}$ accumulated at constant σ_ℓ stress within the cycle duration. The assumed stress σ_ℓ cannot fall below the primary pressure stress σ_p . For stress histories including cycles into the plastic ratcheting regime, the plastic ratchet strain increments calculated using Eqs. (16) and (18) must be added to the creep-induced strain calculated for the mid-wall stress history.

For viscoelastic materials (creep rate proportional to stress) relaxation occurs at a constant total strain through the wall, and the related inelastic strain increment is:

$$\delta = \frac{1}{E}(\sigma_c - \sigma_\ell) \quad (19)$$

However, for the general nonlinear viscoelastic materials of interest, non-uniform relaxation may result in a net total strain increment through the wall. The effect of enhanced creep due to the residual thermal stresses must be added. The enhanced creep was bounded by the authors using energy principles. This strain increment bound is given by:

$$\delta_{(n)} \leq \frac{1}{E} \frac{\sigma_c^2(n) - \sigma_\ell^2(n)}{\sigma_\ell(n)} \quad (20)$$

Note that the use of enhanced creep for a stress level of $\sigma_{\ell(n)}$ is equivalent to treating $\sigma_{\ell(n)}$ as a primary stress during the cycle. Therefore, if the assumed relaxation stress level $\sigma_{\ell(n)}$ is higher than the actual relaxation level, this method conservatively adds the maximum possible additional strain that could occur at the higher assumed level.

On the other hand, suppose that the assumed relaxation level is lower than the actual level to which the stresses relax. In such a case, the energy solution (Eq. 20) includes the maximum possible strain that could possibly occur due to the additional amount of relaxation which was assumed.

Thus, the summation of the strain given by Eq. (20) plus the creep strain at a sustained stress level of $\sigma_{\ell(n)}$ during the cycle gives the maximum possible creep-induced strain that could occur during the cycle for any arbitrary assumed relaxation level, $\sigma_{\ell(n)}$. The choice of $\sigma_{\ell(n)}$ can therefore be varied to minimize the resulting upper bounds on accumulated strain.

One complication is introduced when intermittent severe cycles are followed by less severe cycles. The relaxation level which is assumed for the severe cycle, $\sigma_{\ell(n)}$ may be higher than the core stress for the subsequent cycle, $\sigma_{c(n+1)}$. In such a case, the additional bounded strain due to relaxation from $\sigma_{\ell(n)}$ to $\sigma_{c(n+1)}$ must be added:

$$\delta_{(n+1)} = \frac{1}{E} \frac{\sigma_{\ell(n)}^2 - \sigma_{c(n+1)}^2}{\sigma_{c(n+1)}} \text{ when } \sigma_{\ell(n)} > \sigma_{c(n+1)} \quad (21)$$

The total inelastic strain accumulated during the life of the element is bounded by the sum of the components previously described:

$$\sum \epsilon_{(n)} = \sum [v_{(n)} + \delta_{(n)} + \delta_{(n+1)} + \eta_{(n)}] \quad (22)$$

Where $v_{(n)}$ is obtained from the isochronous curves at the constant $\sigma_{\ell(n)}$ stress levels during each cycle. The relaxation strains $\delta_{(n)}$ and $\delta_{(n+1)}$ are bounded by Eqs. (20) and (21) respectively. The plastic ratcheting strains $\eta_{(n)}$ are given by Eqs. (16) and (18).

CONCLUSIONS

The present analysis extends the applicability of the simplified strain bounding methods given in Code Case 1592 of the ASME Boiler and Pressure Vessel Code to include the beneficial effects of isotropic or kinematic material hardening and the temperature dependence of the yield strength of the material.

New bounding methods are derived by considering the partial relaxation of residual stress fields and applying energy dissipation concepts. These solutions include the effects of enhanced creep. They are quite useful for loading histories which include limited intermittent cycling into the plastic ratcheting regime.

These new bounds eliminate the unconservatism in the complete relaxation formulas given by Bree in Ref. [2]. As Bree pointed out, these formulas do not include the enhanced creep strains.

ACKNOWLEDGEMENT

The solutions reviewed herein were obtained under sponsorship of the High Temperature Structural Design Program of the Oak Ridge National Laboratory. The helpful guidance of J. Corum, T. Yahr and W. Sartory is gratefully acknowledged by the authors.

REFERENCES

- [1] O'Donnell, W. J. and Porowski, J. S. "Upper Bounds for Accumulated Strains Due to Creep Ratcheting," Trans. ASME, Journal of Pressure Vessel Technology, Vol. 96, p. 126 (1974); also Welding Research Council Bulletin No. 185 (1974).
- [2] Bree, J., "Elastic-Plastic Behavior of Thin Tubes Subjected to Internal Pressure and Intermittent High-Heat Fluxes with Application to Fast-Nuclear-Reactor Fuel Elements," Journal of Strain Analysis, Vol. 2, p. 226 (1967).
- [3] Bree, J., "Incremental Growth Due to Creep and Plastic Yielding of Thin Tubes Subjected to Internal Pressure and Cyclic Thermal Stresses," Journal of Strain Analysis, Vol. 3, p. 122 (1968).
- [4] Porowski, J. S. and O'Donnell, W. J., "Upper Bounds for Creep Ratcheting in Convolute Bellows," presented at ASME/CSME Pressure Vessels and Piping Conference in Montreal, Canada (June 1978). Proceedings, Vol. PVP-PB-029, edited by R. S. Barsoum, Simplified Methods in Pressure Vessel Design, p. 15.
- [5] ASME Boiler and Pressure Vessel Code, Code Case 1592-12.

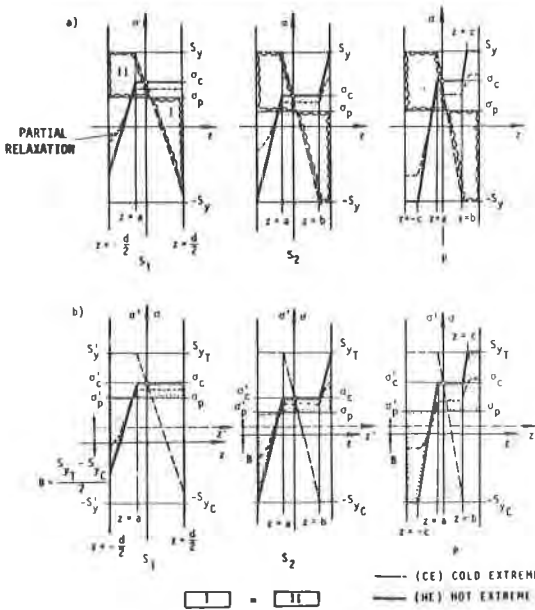


FIGURE 1 STRESS PROFILES AT HOT AND COLD EXTREMES OF THERMAL CYCLE

- a) THE SAME PLASTIC STRENGTH IN TENSION AND COMPRESSION ($B = 0$)
- b) DIFFERENT TENSILE AND COMPRESSIVE YIELD LIMITS ($B \neq 0$)

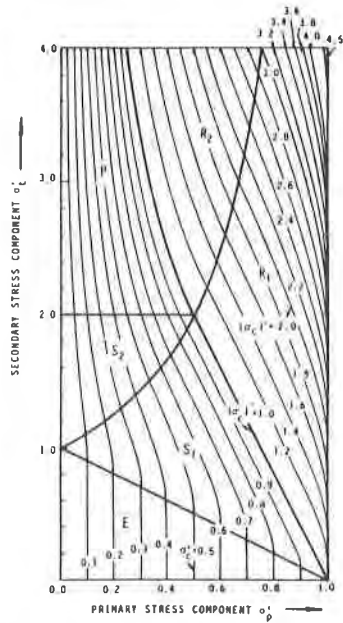


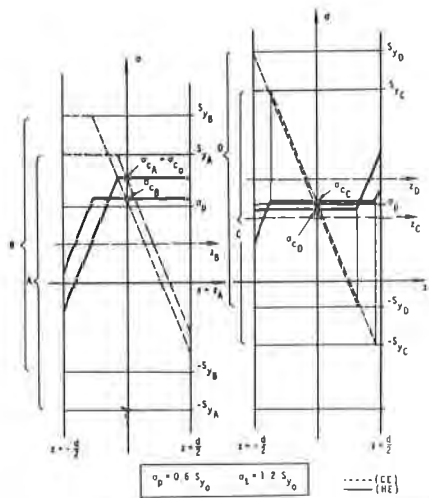
FIGURE 2 GENERALIZED CORE STRESS GRAPH

$$\{\sigma_c\}' = 1 + \sigma_t' - 2\sqrt{\sigma_t'(1 - \sigma_p')}$$

in Regime R_1

$$\{\sigma_c\}' = \sigma_p' \cdot \sigma_t'$$

in Regime R_2



- A $S_{yT} = S_{yC}$ (virgin material) (S_1) REGIME
 B. $(S_{yT} - S_{yC})/2 = 0.3 S_{yO}$ (S_1)
 C. $(S_{yT} - S_{yC})/2 = 0.5 S_{yO}$ (S_2)
 D. $(S_{yT} - S_{yC})/2 = 0.8 S_{yO}$ (S_1)

FIGURE 3
 KINEMATIC HARDENING RESULTS IN LOWER STRESSES IN ELASTIC CORE

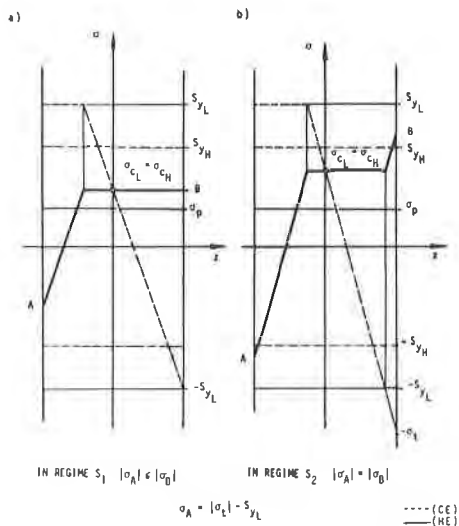


FIGURE 4
 ELASTIC CORE STRESS GENERATED AT LOW TEMPERATURE EXTREME CANNOT EXCEED THE YIELD STRENGTH AT THE HOT EXTREME OF THE CYCLE ($\sigma_{CL} < S_{yH}$)

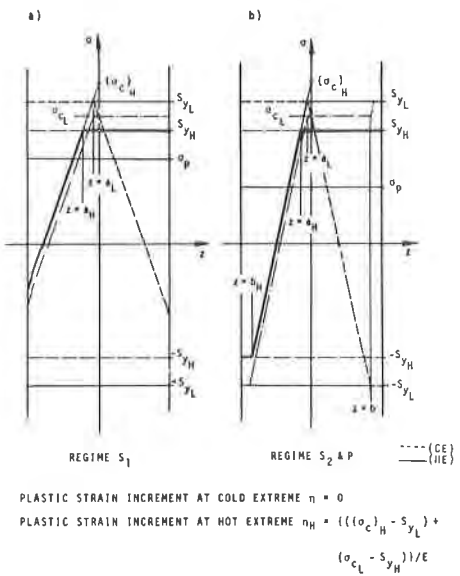


FIGURE 5
 PLASTIC RATCHET AT HIGH TEMPERATURE EXTREME OF THE THERMAL CYCLE

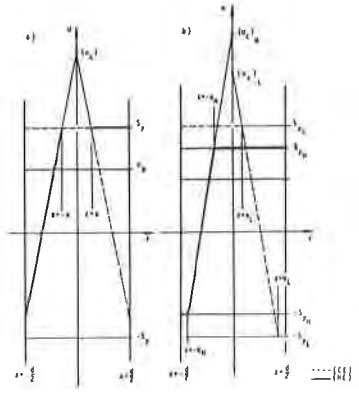


FIGURE 6
 STRESS PROFILES IN RATCHETING REGIMES
 a) REGIME R_1 - CONSTANT YIELD STRENGTH WITHIN A CYCLE
 b) REGIME R_2 - DIFFERENT YIELD STRENGTHS AT BOTH EXTREMES

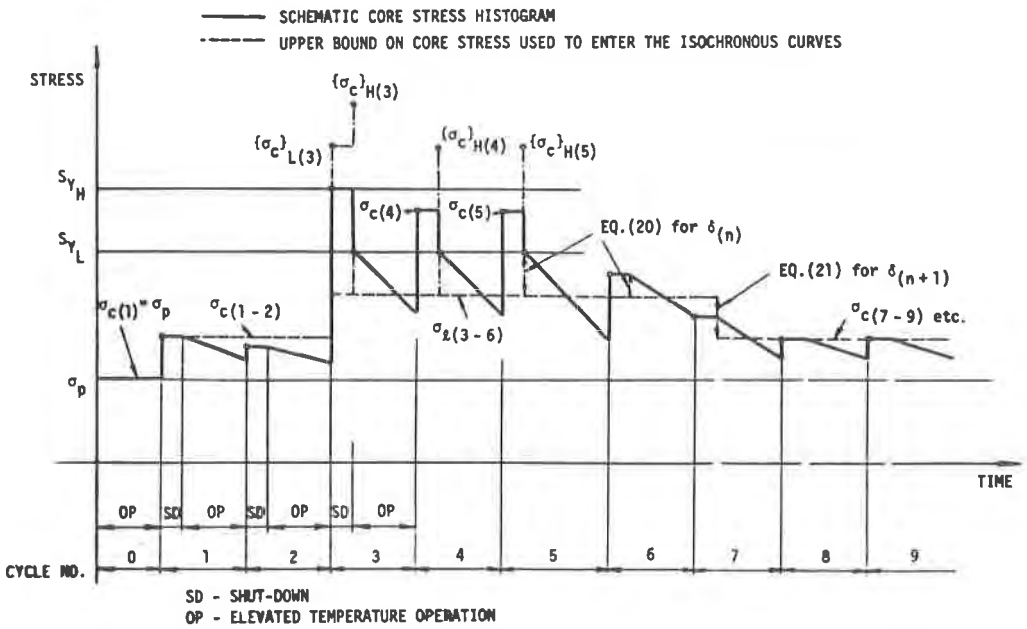


FIGURE 7 SAMPLE CORE STRESS DIAGRAM FOR BOUNDING STRAINS